

Optimization Finite Element Analysis of 3D Spur Gears of Steel and Cast-Iron Reinforced Angles

¹Ifeoluwa E. Elemure, ²Edwin A. Oshin, ³Temitope V. Adebawo, ⁴Aderinsola M. Olawumi, ⁵James O. Akinyoola

¹Department of Mechanical and Design Engineering, University of Portsmouth, UK

²Department of biomedical engineering, Old Dominion University, USA

³physics department, Federal University of Agriculture, Makurdi

⁴Department of Physics Electronics, Federal University of Technology, Akure, Nigeria

⁵Department of Mechanical & Mechatronics, Engineering, Afe Babalola University, Ado-Ekiti, Nigeria

Abstract:- In this research, spur gears made from graphite epoxy normal and shear stresses are examined. The stresses of spur gear are calculated from outer to interior divided into three zones for different angles reinforcement fibres. 3D finite element model (FEM) was used in this study. Also, a novel design, model, and analyse the differential gears by using composite materials. The manual transmission consists of cast iron or mild steel. Composite materials may be an alternative to conventional materials due to the advantages of low weight, rust and less maintenance. Modelling spur gears performed by stable applications and finite element analysis will be performed in Ansys. Eight-node three-dimensional isoperimetric elements are chosen as the finite element method. In the study calculation of normal and shear stresses in different fibre reinforcement orientations has been carried out and are plotted in the graphs. From the analysis, results suggest the use of short reinforcing fibre (SCF) instead of cast iron or mild steel for applications that are limited weight below 1,500 watts. The results of plotting graphs are examined. The force applied to the surface of the first gear orthotropic consisting of the normal stresses of the internal gear. It is higher by about 30%, and the stress value is close to each other.

Keywords:- Spur Gear; Composite Material; Stress Analysis; FEM; Steel; Cast Iron.

I. INTRODUCTION

The principal function of gear mechanisms is to transmit rotation and torque linking bar axes. The gear veer is an apparatus element with the intention of has intrigued many engineers since of numerous technological problems arising in a Complete mesh cycle [1]. In order to realise distinguished load transportation, room with the cut-rate consequence of gear drives, but with Increased strength of gear transmission, gear design based on tooth stress analysis, tooth modifications and Optimum design of gear drives are apt major investigate areas [2]. Gears with involute teeth are inflicted with widely been used in the industry sense of the low cost of manufacturing. The distinguished performance of the gear transmission logic is Obtained through the unique quality of involute gears. The different methods of production of gears, hobbing is the Generally widely useful manufacturing process pro the Construction of involute gear in the industry, [3-5]. Inside

this multi-flank poker chip formation tools often get to the tool life due to unwarranted wear from the tool corner radius [6]. This community wear limits the usable tool Life in run production. Furthermore, the tool wears correlated. Problems cannot be considered all through the design period of spur gears. Some authors are inflicted with been investigated the hob Geometry, cold forces measurements, the poker chip formation Process all through machining and the tool wear prediction [7]. Moreover, several authors urban various simulations Codes of the gear hobbing process, such as SPARTpro and 3D software, [8]. Gear analysis is one of the generally outstanding issues in the apparatus elements theory, particularly in the meadow of gear Design and gear manufacturing. Many of the researchers are inflicted with projected several concepts of pro gear design Optimization to enhance the performance of gear systems. [9,10]. Recently metal matrix composite (MMC) equipment is used to manufacture a digit of engineering components, due to their unique advantages, such as light consequence, unique strength, privileged dimensional Stability and deterioration resistance, as compared with polymer-based composite equipment, though the cost of MMCs is very distinguished. [11,12] Power transmission gears are lone such can get on to aid of MMC equipment. Al- SiC composite can be manufactured by stir casting, and it provides increased resistance and tensile strength with much reduced in consequences [13]. In addition to being lightweight composite materials are both very high strength properties, which of materials use the area more and more. It is expanding. Composite materials, air and land and sea transport in addition to the space industry, chemical industry they are corrosion resistant electrical and electronics insulator) industry, robot construction (less inertia and they are rigid), medical supplies, sports equipment. Such as are used in various fields. It is diversity in the composite material. Due to the option of creating unlimited will further increase is an indisputable fact. Power transmission properties of composite materials It has also shown itself in gear, and the first carbon including a wide variety of fibre composite gears responding to the need of using fibre supplements composite gears are obtained. This desire of gear Even though many of the best features of this Scientific studies in the field are not enough. Experimental and isotropic gear in the literature, theoretical studies are many.

Again, a similar It is aimed, [14] glass- epoxy, and the isotropic steel and cast-iron material made spur of the use in power transmission. They examine and steel and cast-iron best features They concluded owned. Stresses the composite spur gear analysis with the 3D finite element method they did [15] multiple fibre BOND angle in the composite polymer gears they have emphasised stress. In this study; graphite fibre composites straight gear a variety of three defined regions from outside to inside normal and the shear angle formed in the fibre reinforcement, stress applying the finite element method it was examined [16].

II. FINITE ELEMENT METHOD

Three-dimensional investigations; x, y and z-axes, the gear tooth thickness, tooth height and tooth obtained by placing across the width geometry is based. A curvilinear tooth geometry structure because it has eight-node isoperimetric cubic element I₈ was used [18]. The spur gear only Calculations are made based on a tooth. It is only the dental geometrise finite element-boundary sensitive regions separated smaller element precision worked to catch. x and y are placing the resulting two-dimensional finite axis element z-axis perpendicular to the axis of the network team placing the resulting three-dimensional finite element mesh otherwise. Fifty-six elements and 120 nodes in

Analysis point is used. The global stiffness matrix dimensions 360 x 360 and has been according to bandwidth appeared as 141 [19,20].

A. Element Stiffness Matrix

Strain energy in a single element,

$$\pi = \frac{1}{2} \iiint \epsilon^T d\epsilon dx dy dz \tag{1}$$

Here, {ε} is the vector strain displacement vector,

$$\{\epsilon\}^T = \left\{ \frac{du}{dx}, \frac{dv}{dy}, \frac{dw}{dz}, \frac{du}{dy} + \frac{dv}{dx}, \frac{dv}{dz} + \frac{dw}{dy}, \frac{dw}{dx} + \frac{du}{dz} \right\} \tag{2}$$

Here; u, v and w for displacement in x, y and z is formed along the axis of displacement of It is. Elastic matrix for orthotropic material. It shaped. Here, the terms used, E1, E2, E3 values selected according to the fibre direction the axes respectively 1, t, z directions modulus of elasticity are. The values It, TZ, shifts in LZ plane modulus and Poisson's ratio.

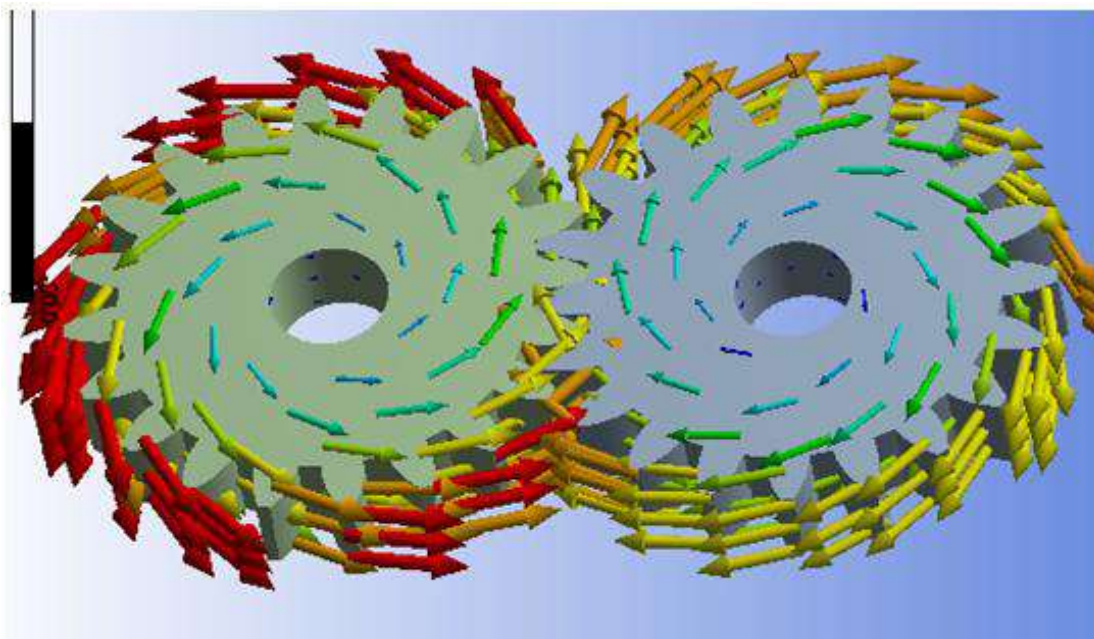


Fig 1:- Shows a Layer Average Vector Rotational Direction Movement

Steel and cast iron material properties in Table I describe Composite Material Features Used

Feature	Steel and cast iron
First Principal Strain (E1)	180994.5 N/mm2
Third Principal Strain (E2)	10702.7 N/mm2
Young modulus (G12)	7171.1 N/mm2
Poisson Ratio (V12)	0.28

Table 1:- Composite Material Used Features

Fibre direction is given these values [T] using the transformation matrix, x, y, z It reached the value in the direction. The maximum contact stress at Hertz stress of compressive stress and contact pressure,

$$P_{max} = \sigma_H = \frac{4F}{\pi BL}$$

Where Contact width

$$B = \sqrt{\frac{8 \times F}{\pi \times L} \times \frac{\frac{1 - \nu_1^2}{E_1} + \frac{1 - \nu_2^2}{E_2}}{\frac{1}{D_1} + \frac{1}{D_2}}}$$

Where, F = Applied Force D1 & D2 = Diameters of the gears, E1 & E2 = Moduli of Elasticity of gear materials, ν_1 = Poisson's ratios of gear materials. [T] matrix = c and h = it is $\sin \alpha \cos \alpha$. [T] transformation matrix and composite materials, elastic matrix ([D]) Include

$$[D^*] = [T][D][T]^T$$

$$\{\epsilon\} = [B]\{U\}$$

Using the matrix obtained by writing equations, the conversion is achieved. Strain matrix given in Equation 2 can be written as follows [12]. Here [B] displacement-strain transformation matrix and {the} nodes spot the displacement vectors. [B] Displacement-way changing the transformation matrix. It shaped the Jacobian matrix functions derivative it is the matrix. Gear having the geometry of curvilinear Due to the three-dimensional, 8-node isoparametric cubic elements were used. This element shape functions

$$N_i = \frac{1}{8}(1 \mp \epsilon)(1 \mp \eta)(1 \mp \xi) \quad i = 1, 2, \dots, 8 \quad (8)$$

Obtained from Eq. Where ϵ , η and ξ axis local coordinates, x, y and z-axes of the global It refer to coordinates. Local coordinates The written equations Jacobi matrix ([J]) is a global It is converted to the coordinates. Therefore, the following equality can write:

$$[K] = \iiint \epsilon^T D^* \epsilon \, dx \, dy \, dz \quad (9)$$

$$= \iiint [B]^T D^* B \, \det[J] \, d\xi \, d\eta \, d\tau$$

Obtained in local coordinates for each element Incorporating global stiffness matrix It was obtained. Using global stiffness matrix substitutions

$$[K]\{U\} = \{F\} \quad (10)$$

Calculated using the equation in [9]. The displacement vector of the system {F} vector is a force acting on the system. Force vector by a uniform load of the node It was obtained by dispersing. So load node points were collected.

B. Method of FEA

The methodology to be followed was adopted to achieve the objective of developing a 3D gear model using solid work. The model was developed and turned into a model of excellent, straight gear elements and solved the same using Ansys and to determine the bending and contact stresses of different gears of straight teeth. Compare the results of different materials and finish the observations

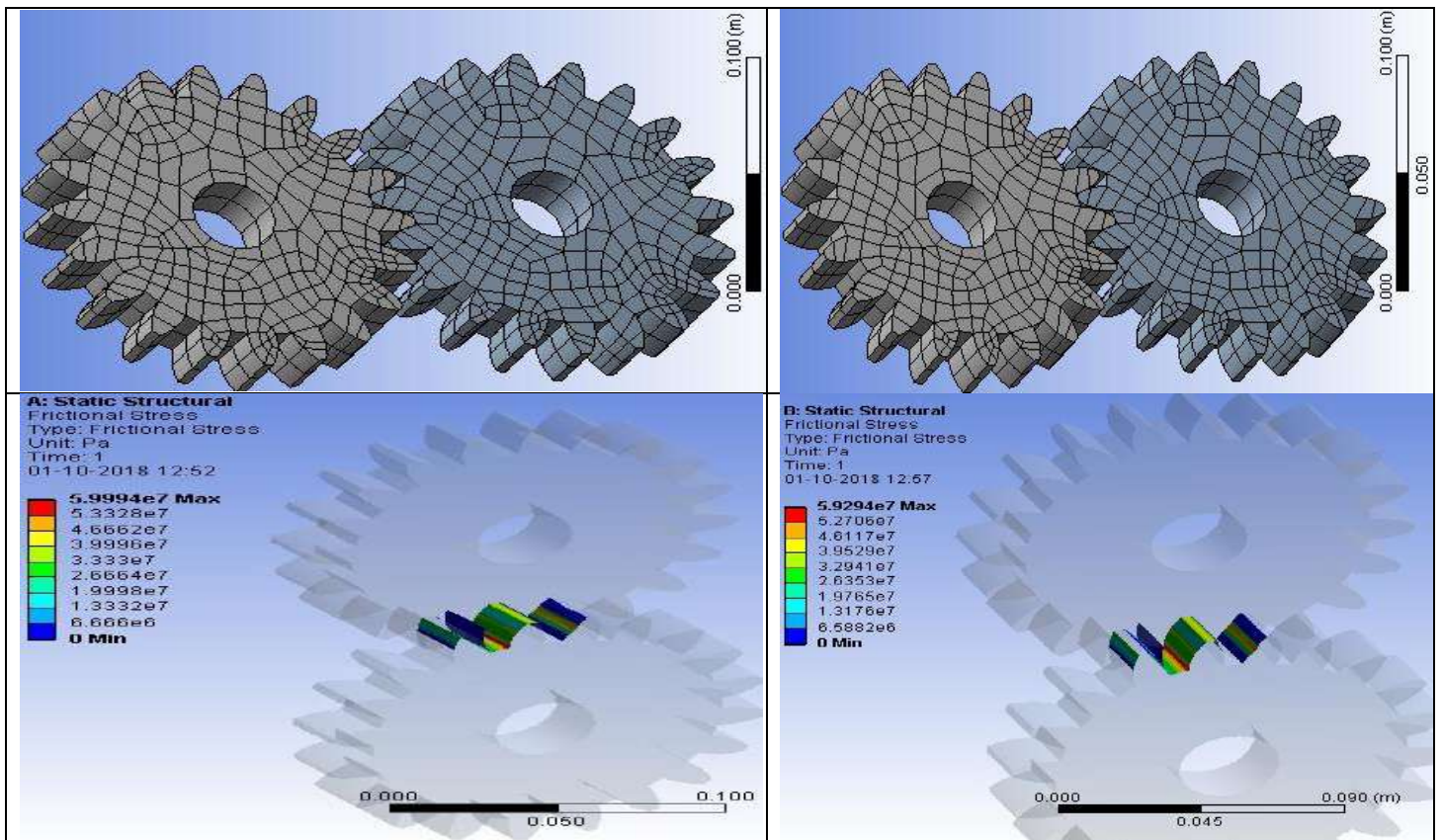


Fig 2:- The Finite Element Method of a Single Tooth Spur Gear of Steel and Cast Iron Reinforce Angle Application.

Dental load distribution across the width (W) $F/W = 150 \text{ N/mm}$. Spread the load is static, and the tooth tip effect was adopted. Clutch along the line The impact load(F) to the outer end, the clutch angle dependent α 'y as it is divided into radial and tangential components. The tangential component of the load $F_x = F \cos\alpha$ Radial Components of them in the form $F_y = F \sin\alpha$. Equality found ten displacement vectors and stress matrix considering equality 6 It can be written as follows.

$$\{\sigma\} = [D][B]\{U\} \tag{11}$$

Stress matrix open

$$\{\sigma\}^T = \{\sigma_{xx} \ \sigma_{yy} \ \sigma_{zz} \ \tau_{xy} \ \tau_{yz} \ \tau_{xz}\}$$

As written. Where σ_{xx} , σ_{yy} , σ_{zz} terms normal stresses τ_{xy} , τ_{xz} , τ_{yz} , per cent In terms slipping It shows the stress.

III. STRESS ANALYSIS OF GEAR

Steel and cast-iron spur gear belonging parameters It is given in Table 2.

Parameter	Value
Pressure angle	20°
Module	12.7 mm
Head height Tooth	1.0mm
Tooth bottom height	1.2mm
Tooth root curvature	0.35mm
Tooth width (W)	3mm
The number of teeth	20

Table 2:- Parameters of Spur Gear.

Made of steel and cast-iron spur are one on female x, y, z-direction standard stress per cent, the shear stresses in the x-y, xz, yz planes respectively. This stress of teeth right and left the centre is divided into two main areas, including It was obtained for each region obtained. First In front of the region upward from below 1, 5, 9, 13, 17, 21, 25'node element is on the back side again bottom-up towards 29, 33, 37, 41, 45, 49, 53'node the elements have been ranked. The second of the elements by adding 1 to the first number of elements, obtained by adding the elements of the third region two they are numbered based on the order. On element in the region of the front and rear Stresses in only the front side is the same element based on the I, II, and III. About the region graphs were drawn. Stresses the same loading in case of and in terms of different fibre reinforcement (0°, 15°, 30° ... 90°) It was calculated. Then the reinforcing fibre direction (First direction) and in the other two directions perpendicular to this direction, (t and z) the usual stresses and I_t , T_Z , I_z shear stress in the plane

were found. These values are different for different angles supplements. It is shown separately calculated and graphics. The force applied to the outer surface of the composite gear σ_x stresses II. The tension in the region It is more than 30% — however, II. and III. Area stress difference between the stresses is minimal. Σ largest areas σ_x strain 30o and 45o have taken place in terms of reinforcing them is 0°, 15° 60° 75° and 90° reinforcement is followed angles (Figure 3). σ_y A little stress is higher than the 90°, 75°, 60°, 45°, 30°, 15° and 0° follow fibre reinforcement angles I. Stress values applied force max in the first region (160N/mm²) as It is realized in the second of 100 N/mm², In the third of 90N/mm². Σ_x as with the stress σ_y of the I and II in the stretching. Between regions stress differences are high, it is next II. and III. Area stress differences have emerged as very small. σ_z stresses σ_x and σ_y small by stress. It has value. For example; In the first of σ_x and σ_y maximum values of stress were 60N/mm² and 160N/mm² while σ_z maximum stress 33N/mm² 'dr. σ_z stress values higher than small to 45°, 30°, 60°, 15°, 0°, 75° and 90° fibre reinforcement angles realised. σ_z and σ_w stresses that show the same value σ_w charts also shown. The most significant σ_L strains 75 and 90 fibre reinforcement It has emerged in the angles. , The remaining terms of supplements ranking 45°, 30°, 15°, 0°, I_t shaped. The maximum in the region stress values is around 140 N/mm², 75 N/mm² and 70 N/mm².

IV. RESULTS

Normal stresses in x, y, z-direction and shear stresses in xy, yz, xz planes were found on a single tooth of the steel and cast iron spur gear. These stresses; It was obtained for each part of the tooth obtained by dividing into two central regions in the middle, on the right and left. In the front of the first region, the elements 1, 5, 9, 13, 17, 21, 25 are arranged from bottom to top, and the elements 29, 33, 37, 41, 45, 49, 53 from the bottom to the rear. The elements of the second region are numbered according to the order obtained by adding the element numbers 1 to the first region and the elements of the third region by adding 2. Since the stresses on the front and rear elements of the regions are the same, only the front elements are based on I., II., And III. Graphics related to the region were drawn. Stresses were calculated at the same loading state and different fibre reinforcement angles (0°, 15°, 30°, ... 90°). Then, normal stresses in the fibre reinforcement direction and two other directions (t and z) perpendicular to this direction and shear stresses in the I_t , T_Z , I_z planes were also found. These values are calculated separately for different reinforcement angles and are shown graphically. The σ_x stresses on the force-applied outer surface (I. zone) of the composite gear II. 30% higher than the stresses in the region. However, II. and III. Stress differences between the region stresses are minimal.

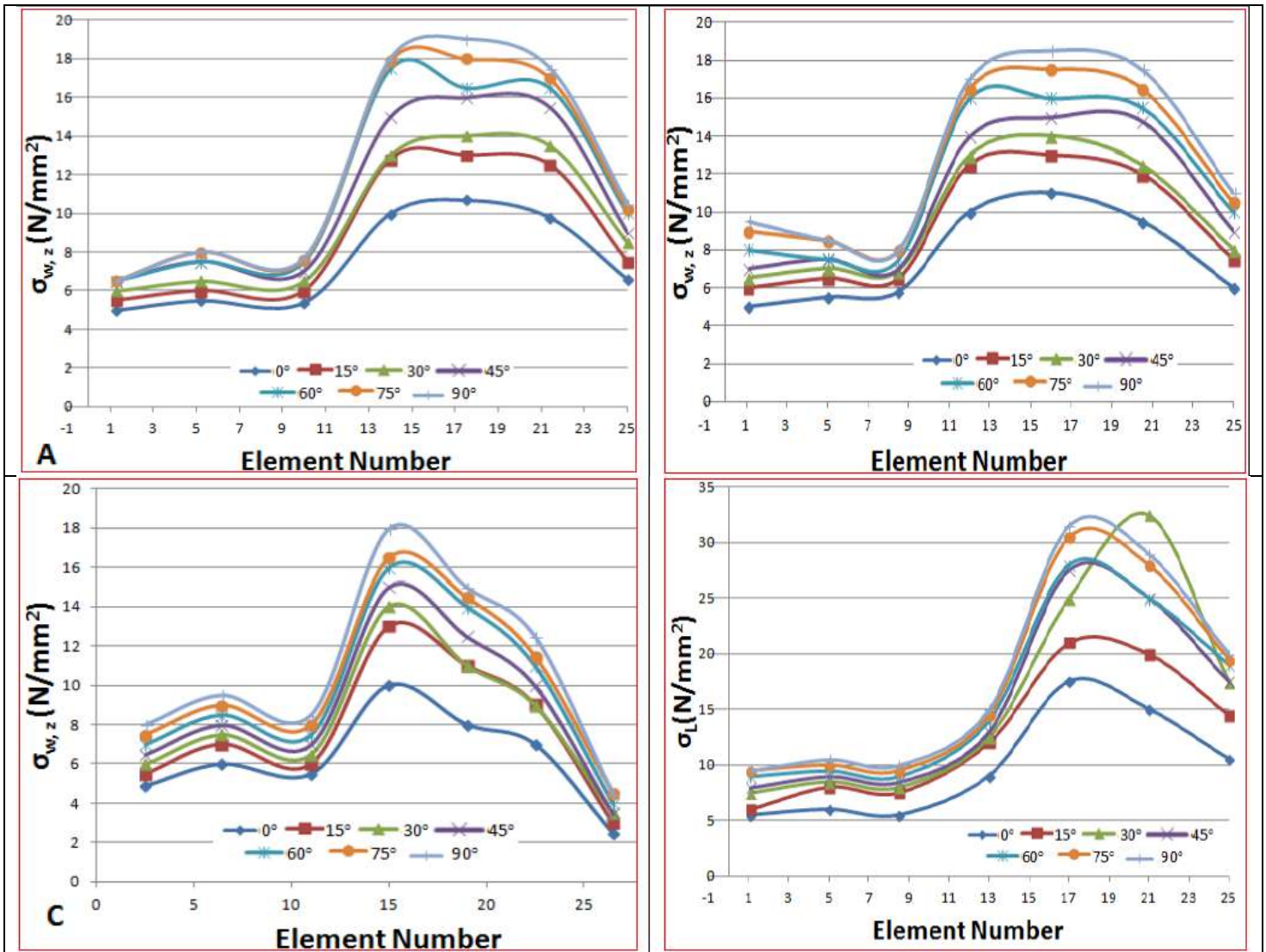


Fig 3:- σ Reinforcement in Composite According to Different Gears in Different Regions z of (A) I, (B) II, (C) III, and (D) σ_L Stresses

The largest σ_x stresses in the regions occurred at 30° and 45° reinforcement angles, followed by reinforcement angles of $15^\circ, 60^\circ, 0^\circ, 75^\circ$ and 90° . σ_y stresses followed by fibre reinforcement angles of $60^\circ, 75^\circ, 45^\circ, 90^\circ, 30^\circ, 15^\circ$ and 0° from large to small. Stress values were maximum 60N/mm^2 in the first region where the force was applied and decreased to 100N/mm^2 in the second region and 90N/mm^2 in the third region (Figure 5). As in σ_x stresses, in the σ_y stresses, The I₁ region and II. Stress difference between the regions is large, besides II. and III. Region stress differences were minimal. The σ_z stresses are smaller than the σ_x and σ_y stresses. For example; The maximum values of σ_x and σ_y stresses in the first region are 60N/mm^2 and 160N/mm^2 , while the maximum stress of σ_z is 33N/mm^2 . Stress values σ_z were observed at $45^\circ, 30^\circ, 60^\circ, 15^\circ, 0^\circ, 75^\circ$ and 90° fibre reinforcement angles from large to small. Since σ_z and σ_w stresses show the same values, σ_w graphs are not shown separately. The greatest σ_L stresses

occurred at 75° and 90° fibre reinforcement angles. 60° followed immediately. The remaining reinforcement angle sequence is $45^\circ, 30^\circ, 15^\circ$ and 0° . The maximum stress values in the regions were approximately $140\text{N/mm}^2, 75\text{N/mm}^2$ and 70N/mm^2 respectively. σ_T stresses were $45^\circ, 30^\circ, 60^\circ, 15^\circ, 75^\circ, 0^\circ$ and 90° . This sequence is the same in all three regions of the gear. Stress values in the regions are $160\text{N/mm}^2, 95\text{N/mm}^2$ and 90N/mm^2 , respectively. The shear stresses τ_{xy}, τ_{lt} and τ_{lw} shown in Figure 9 are obtained for the first region. II. Moreover, III. Since the shear stresses in the regions are much smaller, it is not necessary to put the graphs. The results show that the maximum shear stress τ_{xy} is 125N/mm^2 , while the maximum shear stresses τ_{yz} and τ_{xz} is 3N/mm^2 and 3.5N/mm^2 , respectively. The shear stress τ_{lt} is greater than τ_{tw} and τ_{lw} . The shear stresses of τ_{lt} have positive values at $15^\circ, 30^\circ$ and 0° fibre reinforcement angles and negative values at $45^\circ, 90^\circ, 75^\circ$ and 60° fibre reinforcement angles.

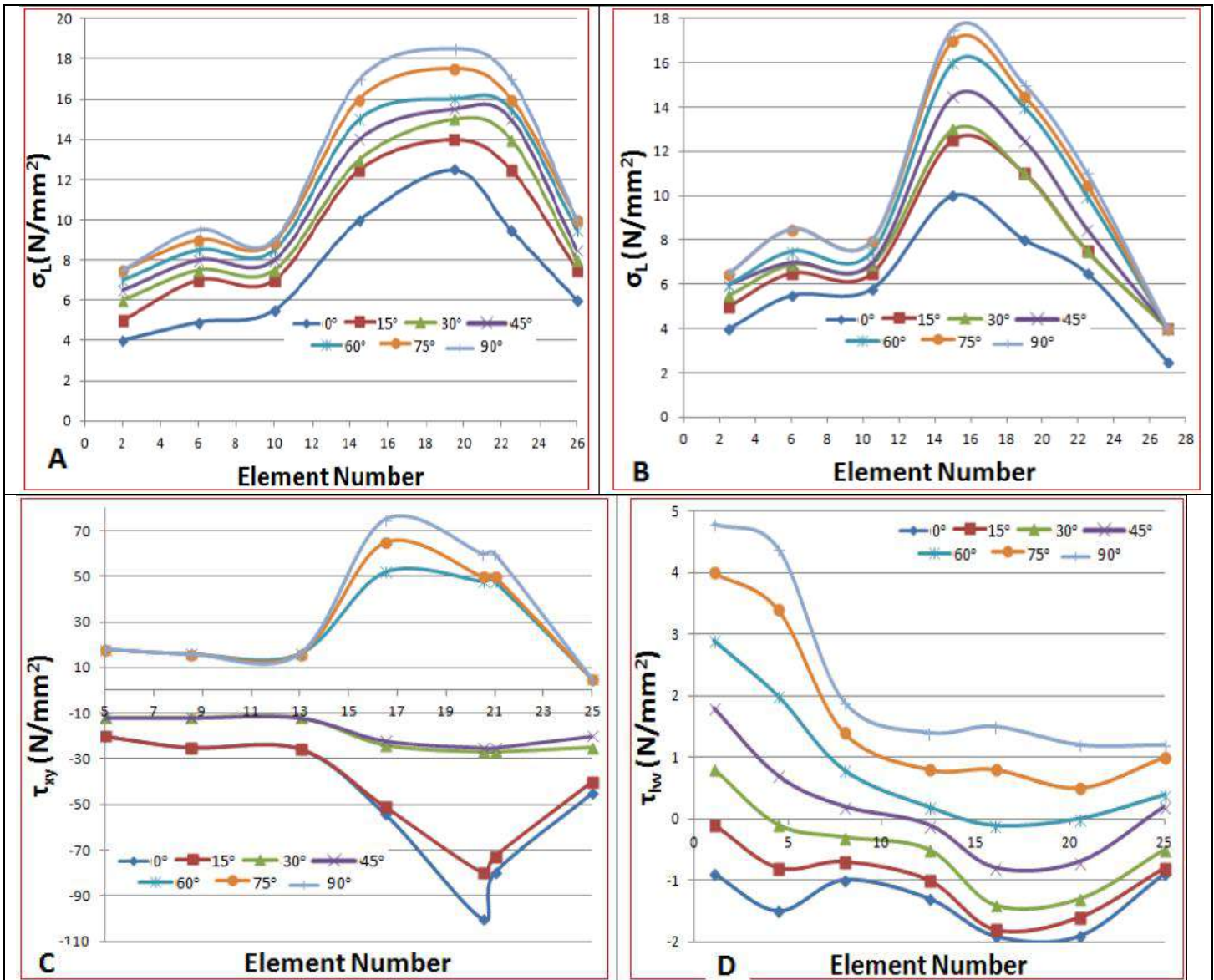


Fig 4:- σ_L According to Different Supplements in the Different Regions of (A) II, (B) III, τ According to Different Supplements in Different Regions of the Composite Gear (C) τ_{lt} (D) τ_{lw}

➤ *Finite Element Analysis*

The finite element analysis of the spur gear is performed in the ANSYS 14, a popular FEA tool. Within the structure of the mechanical engineering discipline (such as the aerospace, biomechanics and automotive industries), several specialisations usually use integrated MEFs to design and develop their products. Some new FEM packages include particular components, such as thermal, electromagnetic, fluid and vertical work environments. In a structural simulation, the FEM is a tremendous help in the production of visualisations of hardness and durability, in

addition to minimising weight, materials and costs. The MEF provides a detailed view of where structures bend or bend and show the distribution of stresses and displacements. FEM software offers a wide range of simulation options to control the complexity of modelling and analysis of a system. In the same way, the desired level of precision and the associated calculation time requirements can be managed simultaneously for most engineering applications. The FEM guarantees that all projects are built, improved and optimised before the project is done.

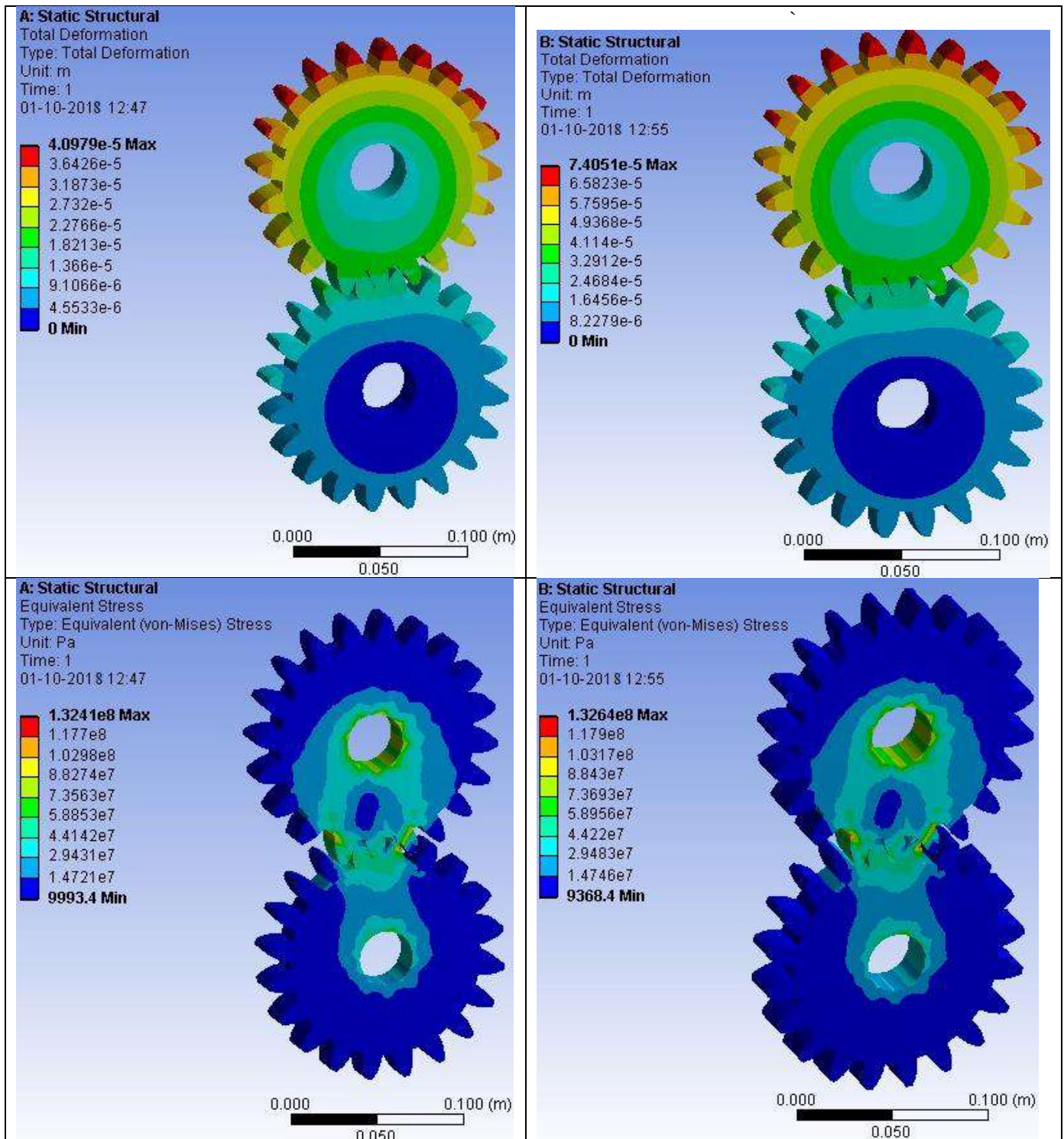


Fig 5:- Finite Element Analysis of

V. CONCLUSION

In this research calculation of normal and shear stresses in different fibre reinforcement orientations has been carried out and are plotted in the graphs. Generally, the maximum value of the τ_{xy} stress occurs at zero degree and 90degree fibre reinforcement angles. The results of plotted graphs are evaluated and discovered that the force applied to the surface of the gear 1 Orthotropic consisting of the normal stresses of the inner gear it is higher by about

30%. The inner gear region (II. And III. Area) The stress values occur very close to each other and a rise in terms of different fibre reinforcement regarding the following stress values results obtained. Also, the maximum values of σ_x stress and σ_y stress occur at 30degree and 45degree and 60degree and 75degree fibre reinforcement angles, respectively. Based on static analysis, we observe that the von Mises stress and the deviation of the gear increase when the pressure on the surface of the blade increases. The voltage received for the helical gears added with the SCF is

below the safety limit compared to cast iron and mild steel. From studies suggesting the use of analytical results and additional gear results, SCF will be the best choice for cast iron gears and mild steel gears in applications with a maximum usage limit of 1500 watts.

REFERENCES

- [1]. P.B.Pawar, Abhay A Utpat, Analysis of Composite Material Spur Gear under Static Loading Condition, MT: Proc 2 (2015) 2968 – 2974
- [2]. C. O. Ijagbemi, B.I. Oladapo, H.M. Campbell, C. O. Ijagbemi, Design and simulation of fatigue analysis for a vehicle suspension system (VSS) and its effect on global warming, procedia engineering 159, 124-132
- [3]. Chabra Pankaj, “*Design and Analysis of Composite Material Gear Box*”, IJMCE, Vol.1(2012), Issue1, pp 15-25
- [4]. Russo R, Brancati R, Rocca E. Experimental investigations about the influence of oil lubricant between teeth on the gear rattle phenomenon. J Sound Vib 2009; 321:647–61
- [5]. De la Cruz M, Theodossiades S, Rahnejat H. An investigation of manual transmission rattle. Proc Inst Mech Eng, Part K: J Multi-Body Dynam 2010;224:167–81.
- [6]. P. Marimuthu, G. Muthuveerappan, Optimum Profile Shift Estimation on Direct Design Asymmetric Normal and High Contact Ratio Spur Gears Based on Load Sharing, Procedia Engineering 86 (2014) 709 – 717.
- [7]. Chawathe D.D, “*Handbook of Gear*”, New Age IP,(2011) pp 26-89,305-536, 579-706
- [8]. Bankole I Oladapo, S Abolfazl Zahedi, F Vahidnia, OM Ikumapayi, Muhammad U Farooq, Three-dimensional finite element analysis of a porcelain crowned tooth, Beni-Suef University journal of basic and applied sciences 7 (4), 461-464
- [9]. Bozca M, Fietkau P. Empirical model-based optimisation of gearbox geometric design parameters to reduce rattle noise in an automotive transmission. Mech Mach Theory 2010;45(11):1599–612.
- [10]. VA Balogun, BI Oladapo, Electrical energy demand modelling of 3D printing technology for sustainable manufacture, International Journal of Engineering 29 (7), 1-8
- [11]. P.B.Pawar1, Abhay A. Utpat, Development of Aluminium Based Silicon Carbide Particulate Metal Matrix Composite for Spur Gear, Procedia Materials Science 6 (2014) 1150 – 1156
- [12]. I Oladapo Bankole, Stephen Aban, M Temitayo Azeez, S Oluwole Afolabi, Computer Aided Drafting and Construction of Standard Drafting Table for College of Engineering Studio in Afe Babalola University, International Journal of Scientific & Engineering Research, Volume 6, Issue 8, August-2015
- [13]. Klocke F, Gorgels C, Herzhoff S. Tool Load during Multi-Flank Chip Formation. Advanced Materials Research, Vol. 223: 525- 534; 2011.
- [14]. N. Sabkhi, C. Pelaingre, C. Barlier, A. Moufki, M. Nouari, Characterization of the cutting forces generated during the gear hobbing process: Spur gear, Procedia CIRP 31 (2015) 411 – 416.
- [15]. B. I Oladapo, B. A Vincent, A. O Oke, E. A Agbor, Design and finite element analysis on car seat height screw adjuster using Autodesk inventor, Int. J. Sci. Res. Eng. Stud. (IJSRES) 2 (8)
- [16]. Antoniadis A, Vidakis N, Fatigue Fracture Parameters on the Level of Tool Stresses-A Quantitative Parametric Analysis, J. Manuf. Sci. Eng., 2002, vol. 124, no, 4, p. 784-791.
- [17]. Tapoglou N et Antoniadis A. CAD-Based Cal of Gear Hobbing, J. Manuf. Sci. Eng., 2012, vol. 134, no, 3, p. 8.
- [18]. Bankole. I. Oladapo, S. Abolfazl Zahedi, Francis. T. Omigbodun, Edwin A. Oshin, Olaoluwa B. Malachi, Microstructural evaluation of aluminium alloy A365 T6 in machining operation, Journal of Materials Research and Technology 8 (3), 3213-3222
- [19]. Kapelevich A L, Geometry and design of involute spur gears with asymmetric teeth, Mechanism and Machine Theory 35 (2000) 117-130.
- [20]. Galaxia Pratik, Awate N.P., “*Design, Modelling & Analysis of Gear Box for Material Handling Trolley: A Review*”, Mechanica Confab, Vol 2, Issue1,(2013),pp63-70.